Hindawi
Geofluids
Volume 2022, Article ID 5690355, 11 pages
https://doi.org/10.1155/2022/5690355

Research Article

The Influence of Buckling Mode and Buckling Stability Coefficient of Rigid-Frame Bridge during Construction in Cold Region

Jiangjiang Li,[1] **Xuanyu Zhang**,[2] **and Xiandong Wang**[1]

[1]*School of Highway, Chang'an University, Middle Section of the South Second Ring Road, Xi'an, Shaanxi 710064, China*
[2]*Shandong Hi-Speed Company Limited, Long'ao North Road, Jinan, Shandong 250000, China*

Correspondence should be addressed to Jiangjiang Li; lijiangjilin@chd.edu.cn

Received 10 November 2021; Accepted 25 March 2022; Published 16 July 2022

Academic Editor: Zhiwei Zhou

The study aims to further standardize the construction process, improve the construction quality, and ensure the stability of infrastructure construction. The continuous rigid-frame bridge is taken as the research object, the finite element model of the bridge body is established by using the beam element, and the overall stability of the rigid-frame bridge is analyzed in the construction and completion stages. Moreover, the stability coefficient and buckling mode are established under different working conditions in each stage, the linear stability variation law is summarized, and the geometric nonlinear stability analysis method is established through the specific data. The nonlinear stability safety factor and buckling mode are obtained, and the influence of wind load and initial defects on the stability of continuous rigid-frame bridge is further explored. The results show that with the increase of the bridge height, the overall stability factor of the bridge is decreasing, and the safety factor of the single-limb thin-walled hollow pier is relatively larger than that of the double-limb thin-walled hollow pier. During the construction, the asymmetric self-weight load caused by the asynchronous load and cantilever pouring has the greatest impact on the stability of the bridge. The stability safety factor of the geometric nonlinear stability analysis method constructed is 0.3% and 1.27% lower than the ideal state, respectively. The stability safety factor of the wind load and the initial defect is 12.65% lower than the ideal state, and the stability safety factor is greatly reduced. The results have important reference significance to ensure the construction safety and overall stability of the bridge.

1. Introduction

With the development of the transportation industry in China roads, the country has performed large-scale infrastructure construction including roads and bridges to meet the growing demand for transport [1, 2]. Particularly, continuous rigid-frame bridge structure has been increasingly widely applied in modern bridge construction, since the cantilever construction of continuous rigid-frame bridge can overcome the complex situation in the construction environment to meet the development trend of long-span and soft bridges. In modern times, continuous rigid-frame bridge combines the characteristics of T-shaped structure and continuous beam bridge, which meets the development of modern bridge construction [3]. Additionally, high piers are used in the process of bridge construction to adapt to the deformation caused by factors such as prestress of bridge superstructure and shrinkage and creep of concrete [4]. When there are influences of hydrogeological and other natural environments on the construction process of continuous rigid-frame bridge, it is necessary to design a short-pier bridge for the large-span continuous rigid-frame bridge structure and to study and analyze the actual stress of the continuous rigid-frame bridge structure [5]. In the construction and completion stages of continuous rigid-frame bridge, the overall stability of the bridge will change, and the stability coefficient and buckling mode of the bridge will also change under different working conditions [6].

Therefore, further analysis is conducted on the stability of the bridge in the construction process to improve the

construction quality of the continuous rigid-frame bridge. Taking the continuous rigid-frame bridge as the research object, the finite element analysis is adopted to analyze the stiffness of continuous rigid-frame bridge with different pier structures, and the nonlinear stability of continuous rigid-frame bridge is studied under construction. Moreover, the buckling stability of continuous rigid-frame bridge under different working conditions is explored to obtain the stability coefficient and buckling steady state of continuous rigid-frame bridge. Ultimately, the influencing factors of the stability of continuous rigid-frame bridge are further studied under different wind loads and initial defects.

2. Literature Review

Both domestic and foreign scholars have conducted related research. Rossi et al. (2020) studied the stability mode changes of lateral deformation buckling and local buckling when steel-concrete composite beam was under negative bending moment and explored the displacement and distortion of the compression flange caused by the deformation of the web during the buckling process. They utilized the lateral torsional buckling theory and the U-frame model to conduct the geometric nonlinear numerical analysis of the composite beam and investigated the strength changes of the composite beam under different negative torques. They found that the cross section and web stiffener are the main parameters affecting the lateral deformation buckling [7]. Rossi et al. investigated the solution of lateral torsional buckling of bridges and analyzed the bridge by classical elastic critical moment theory. They simplified the model by equivalent flange to accurately predict the elastic critical load of bridge. They gained more simplified and accurate bridge slab data than the truss model through the model. Besides, they compared the test results of critical load and design load. Moreover, they studied the transverse torsional buckling of two-span and two-beam steel-concrete composite bridge under the constraint of section size, lateral constraint, and bridge configuration to prove the advantages of the design model [8]. Thanopoulos et al. analyzed the inelasticity of concrete-filled steel tubular piles and soil under cyclic and seismic loads and discussed the overall buckling stability of pile foundation under seismic conditions. They believed that concrete-filled steel tube piles could reduce the irreparable damage of the pile. They studied the buckling state under seismic load by analyzing the nonlinear mechanical behavior of concrete-filled steel tubular piles and the soil-structure interaction effect and modeling based on the control load. They proved that the adopted soil-pile interaction and soil nonlinear model could well analyze the problem through experiments [9]. Serras et al. proved that the formation mode of shear stress in sinusoidal web was the same as that in noncomposite steel beams [10]. Śledziewski and Górecki explored the fatigue crack problem of the top member of the steel truss railway bridge truss due to the high impact load of the passing wheel on the bridge. They used continuous welded track to solve the thermal interaction between the track and the bridge. Meanwhile, they stated that the incorporation of high longitudinal restraint between the track and the bridge would increase the risk of track buckling failure at bridge transition zones, since bridge thermal expansion during hot weather could add compressive forces to the rails transferred through the track fastening system. Their experimental results indicated that providing 50% elastic fasteners and 50% zero-toe load fasteners on each span could alleviate the thermal problems of continuous welded rails on bridges [11].

Previous works have proved that finite element analysis can effectively study engineering nonlinear problems, to further standardize the construction process and improve the quality of the project. However, further analysis is needed for the buckling stability of different types of piers of continuous rigid-frame bridge structure. Therefore, the investigation is performed on the nonlinear stability coefficient and buckling mode of single-limb thin-walled piers and double-limb thin-walled pier under different construction conditions here, along with the discussion of the overall stability of the bridge under wind load and initial defects. Finally, the established bridge model is verified by simulation test.

3. Steady-State Analysis of Buckling of Rigid-Frame Bridge under Construction Condition

3.1. Development and Characteristics of the Continuous Rigid-Frame Bridge. With the development of social economy and the implementation of the rural revitalization strategy, the construction of traffic roads has become an important foundation to accelerate regional economic development, so the construction of infrastructure including roads and bridges has been rapidly expanded [12]. However, it is essential to constrain the route environment, linear index requirements, and construction costs in the concrete construction of roads and bridges, which requires low cost and good structural stability of the bridge construction technology [13]. Long-span continuous rigid-frame bridge is a prestressed bridge structure with the advantages of large stiffness, good integrity, small deformation, and good seismic performance. In addition, the deformation and deflection curve of the girder is flat, providing comfort driving, and there are less expansion joints on the rigid-frame bridge floor. Therefore, the long-span continuous rigid-frame bridge is widely used in the construction of roads and bridges [14].

As a pier-beam consolidation structure, continuous rigid-frame bridge has the stress characteristics of T-shaped structure and continuous beam, which has good spanning capacity and transportation capacity. Besides, the continuous rigid-frame bridge does not need bears, which can avoid large-tonnage pot bears but retain stress characteristics of continuous beam bridge to reduce the cost of the project [15]. The cantilever construction is necessary in the construction process of the continuous rigid-frame bridge, instead of setting the bear on the main pier, which can greatly improve the construction convenience. Moreover, the transverse torsional stiffness and the bending stiffness along the bridge direction of the continuous rigid-frame bridge can also adapt to the actual needs of long-span

bridges [16]. The construction of the continuous rigid-frame bridge is promoted vigorously in the western mountainous area and the construction project of the river-crossing and sea-crossing bridges. In the superstructure of the continuous rigid-frame bridge, the girder adopts high-strength and light-weight concrete to reduce the self-weight of the box girder. Besides, the lightweight upper bridge structure reduces the requirements of the hanging basket and the stress of the lower structure while enhancing the spanning ability of the continuous rigid-frame bridge. Figure 1 presents the application of continuous rigid-frame bridge in road construction.

In the construction process, the boundary cross-fold is realized through the launching nose or cantilevered end connected with the approach bridge under the foundation of an appropriate proportion of side span and main span [17]. For high-pier continuous rigid-frame bridges, the construction cost can be reduced by cancelling the floor support of the side span closure [18]. China's western region is mostly composed of crisscrossed landform such as plateaus, mountains, and ravines, where the ground fluctuates greatly, which requires a high pier height of the bridge, especially when crossing deep water and deep valley. Therefore, the pier height of continuous rigid-frame bridges increases with the increasing demand for western construction [19]. However, in the construction of urban river-crossing bridges, due to the constraints of designed linear elevation, hydrological conditions, and engineering geology, the pier height of continuous rigid-frame bridge is required to be as low as possible [20]. Thin-walled piers are most common in continuous rigid-frame pier structures because they can accommodate the force and deformation requirements of the structure.

3.2. Types of Pier Structure of the Continuous Rigid-Frame Bridges. Continuous rigid-frame bridge is a multiple statically indeterminate structure, and a great additional secondary internal force will be generated within the bridge structure under the conditions of uneven settlement of prestress and bears and shrinkage, creep, and temperature change of concrete. Therefore, the main pier of the bridge is required to have a certain flexibility to form a swing support system for the bridge [21]. In the design process of continuous rigid-frame bridge, the main beam, pier, and foundation are regarded as a whole, so the seismic performance of the bridge is good. When the bridge is subjected to seismic force, the force will be dispersed to each pier, effectively reducing the influence of seismic force on the pier. Therefore, it is not necessary to establish a large-tonnage seismic bear in the construction process [22, 23]. Moreover, the curvilinear bottom is used in the bridge box girder to reduce the size of the bridge structure and ensure the safe flood discharge with a large clearance height under the bridge. Furthermore, expansion joints are designed at the two ends of the bridge instead of the bridge floor of continuous rigid-frame bridge, which requires the expansion displacement of the two ends of the bridge to be consistent. Meanwhile, there is a block for the abutment of the bridge to control the horizontal displacement of the bridge road and ensure the horizontal stability of the bridge.

At present, the common types of piers of continuous rigid-frame bridges include single-limb thin-walled pier, double-limb thin-walled pier, X-shaped pier, V-shaped pier, and Y-shaped pier. The structural section of single-limb thin-walled pier is a solid or hollow rectangular or box girder section. Generally, the single-limb thin-walled pier with box girder section has good torsional resistance and strong thrust stiffness. The cross-sectional area of the single-limb thin-walled pier is similar to that of the double-limb thin-walled pier, but the thrust stiffness of the single-limb thin-walled pier when subjected to force is much stronger than the force on the double-limb thin-walled pier [24]. Hence, the flexibility of the box type single-limb thin-walled pier will be worse under the same conditions, but it can be improved by increasing the pier height of the single-limb thin-walled pier, which can also increase the longitudinal displacement of the bridge top [25]. In the construction of roads and bridges in China's west region, single-limb thin-walled piers are showing increasingly obvious superiority facing increasingly higher piers. Meanwhile, the construction difficulty of single-limb thin-walled piers is lower than that of double-limb thin-walled piers, which has better effect on the establishment of curved bridges. Figure 2 illustrates the single-limb thin-walled pier in mountain engineering construction.

Compared with the structure of single-limb thin-walled pier, the double-limb thin-walled pier divides the wall pier into two parts and sets a certain interval between the two thin-walled piers, so the double-limb thin-walled pier has better thrust stiffness, reducing the thrust stiffness along the bridge and effectively meeting the requirements of the displacement change of the bridge deck. The girder of the double-limb thin-walled pier suffers a smaller internal force than the single-limb thin-walled pier. Besides, since the peak bending moment of the pier top is in the two pier column tops, the bending moment between the two thin-walled piers is also smaller than that of the single-limb thin-walled pier [26]. Therefore, the pier top section size can be minimalized during the design of pier top girder to reduce the consumption of bridge materials. Double-limb thin-walled piers are adopted in the construction of long-span bridges to ensure the strength and stability of the bridge, as well as a small thrust stiffness to solve the displacement problem of the bridge pier top [27]. Like the single-limb thin-walled pier, the cross section of the double-limb thin-walled pier also contains hollow piers and solid piers. Figure 3 shows the application of the double-limb thin-walled pier in the river-crossing project [28]. There are another three types of piers of continuous rigid-frame bridge, namely, X-shaped pier, V-shaped pier, and Y-shaped pier, which all have the characteristics of small main beam height and light bridge structure. Since these three types of pier are not common in practical construction, they are not mentioned in the study. Figure 4 represents a V-shaped pier.

3.3. Analysis of Static Force and Stiffness of Continuous Rigid-Frame Bridges during Construction. In the construction of bridges, it is necessary to study the cross-sectional form of the bridge to reduce the thrust stiffness of

(a) Huatupo Super Bridge of Neijiang-Kunming Railway (b) Qingshui River Bridge of Nanning-Kunming Railway

Figure 1: Application of continuous rigid-frame bridge in road construction.

Figure 2: Single-limb thin-walled pier under construction.

continuous rigid-frame bridge and reduce the interface inertia moment along the bridge direction. In the design of the main pier section, it is required to minimize the size of the cross section along the bridge direction and increase the size of the transverse bridge direction. The pier of continuous rigid-frame bridge usually adopts the hollow solid pier. There is no interspace within solid piers, while hollow piers give full play to the strength of the material and reduce the consumption of building materials [29–32]. At present, the pier of large-span rigid-frame bridge includes single-limb thin-walled solid pier, double-limb thin-walled solid pier, single-limb thin-walled hollow pier, and double-limb thin-walled hollow pier. Figure 5 indicates each structure of these four types of piers.

Under the action of external force, the horizontal displacement pier will occur in the pier of the long-span continuous rigid-frame bridge, and the horizontal force is transferred by the upper structure of the bridge. When calculating the flexibility of the bridge, the generalized displacement of the pier top caused by the unit generalized force on the pier is called the flexibility of the pier under this force, with the unit of δ. Besides, the stiffness is represented by K, and its value is the reciprocal of flexibility, which can be expressed as

$$\delta = \frac{1}{K}. \tag{1}$$

The bending moment at the top of the long-span continuous rigid-frame bridge pier has little effect on the horizontal displacement of the flexible pier, so the angle constraint ability of the main beam of the rigid-frame bridge is weak. Long-span continuous rigid-frame bridge usually adopts pile group foundation or rigid expanded foundation, while the pier body has strong flexible and small stiffness, so it is assumed that the pier and foundation are consolidated [33]. For the calculation of the free cantilever column in the upper section of the bridge, the height of the pier is taken as the distance from the bottom of the main beam to the top of the cap, denoted as l, and Q represents the lateral force on the pier top. Therefore, the strain capacity of the pier can be written as

$$U = \int \frac{M^2}{2EI} dx, \tag{2}$$

$$M = -Qx, \tag{3}$$

where E denotes the elasticity modulus and I stands for the second moment of area, then:

$$U = \int \frac{(-Qx)^2}{2EI} dx = \frac{Q^2 l^3}{6EI}. \tag{4}$$

In the calculation process, according to Castigliano's first

Figure 3: Double-limb thin-walled pier under construction in the river-crossing project.

Figure 4: V-shaped pier.

theorem, the horizontal displacement of the free end can be presented as

$$\delta = \frac{\partial U}{\partial Q} = \frac{Ql^3}{3EI}. \tag{5}$$

When the longitudinal displacement of the bridge is 1, the force used to generate unit displacement is called the thrust stiffness shown as

$$K = \frac{3EI}{l^3}. \tag{6}$$

In the research process, the pier height is l, and the distance between double-limb thin-walled piers is denoted as r. Correspondingly, the thrust stiffness ratio of single-limb thin-walled pier and double-limb thin-walled pier along the bridge direction is

$$K = \frac{3EI}{l^3} = \frac{2Eab^3}{l^3}, \tag{7}$$

$$K = 2 \times \frac{3EI}{l^3} = \frac{Eab^3}{2l^3}. \tag{8}$$

From Equation (7) and Equation (8), the single-limb thin-walled pier has the thrust stiffness four times that of the double-limb thin-walled pier, so the flexibility of the double-limb thin-walled pier is larger, which can effectively solve the longitudinal horizontal deformation caused by the main girder prestress, and shrinkage, creep, and temperature change of concrete of the superstructure of bridges [34]. According to the above description, the along-bridge inertia moments of single-limb thin-walled pier and double-limb thin-walled pier can be expressed as follows:

$$I_a = \frac{a(2b)^3}{12} = 0.667ab^3, \tag{9}$$

$$I_b = \frac{2ab^3}{12} + r^2ab. \tag{10}$$

Substitute r into Equation (10) to obtain the value of I_b to compare it with I_a. The results are shown in Table 1, demonstrating that the double-limb thin-walled pier shows better safety in the cantilever construction process, which can solve the problem of unbalanced bending moments in the construction process.

When the torque of single-limb thin-walled pier and double-limb thin-walled pier under the action of the transverse bridge force is M_r, there will be a torsional angle θ, and the resistance torque generated at the top of the pier is M_{Ta}. When the two-limb thin-walled pier is subjected to the transverse bridge torque, there will be a torsion angle and cross-bridge relative displacement, consisting of the

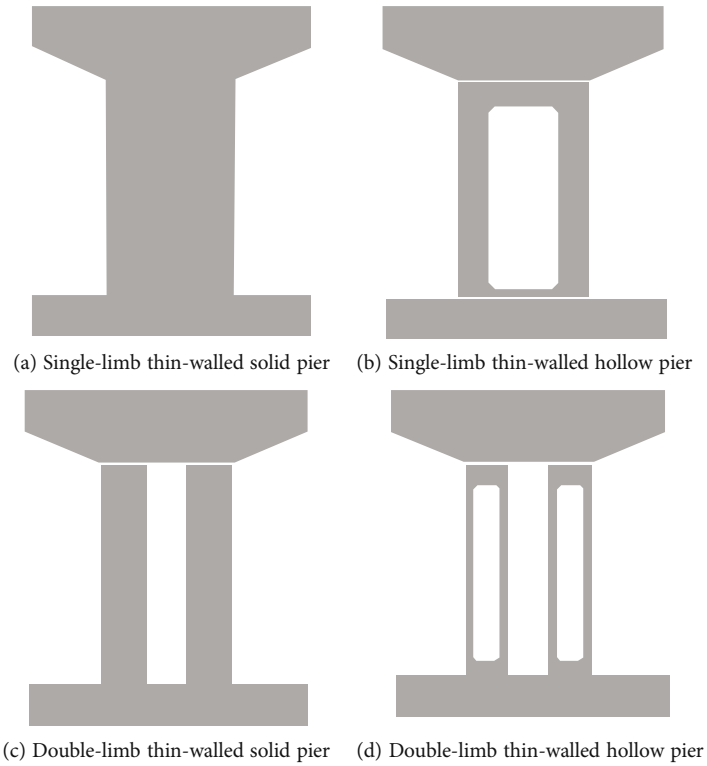

(a) Single-limb thin-walled solid pier (b) Single-limb thin-walled hollow pier

(c) Double-limb thin-walled solid pier (d) Double-limb thin-walled hollow pier

Figure 5: Cross sections of different piers of continuous rigid-frame bridges.

Table 1: Comparison of thrust stiffness of single-limb thin-wall pier and double-limb thin-wall pier.

r	$r = b$	$r = 2b$	$r = 3b$	$r = 4b$
I_b	$1.167ab^3$	$4.167ab^3$	$9.167ab^3$	$16.167ab^3$
Ratio of I_b to I_a	1.75	6.25	13.75	24.2

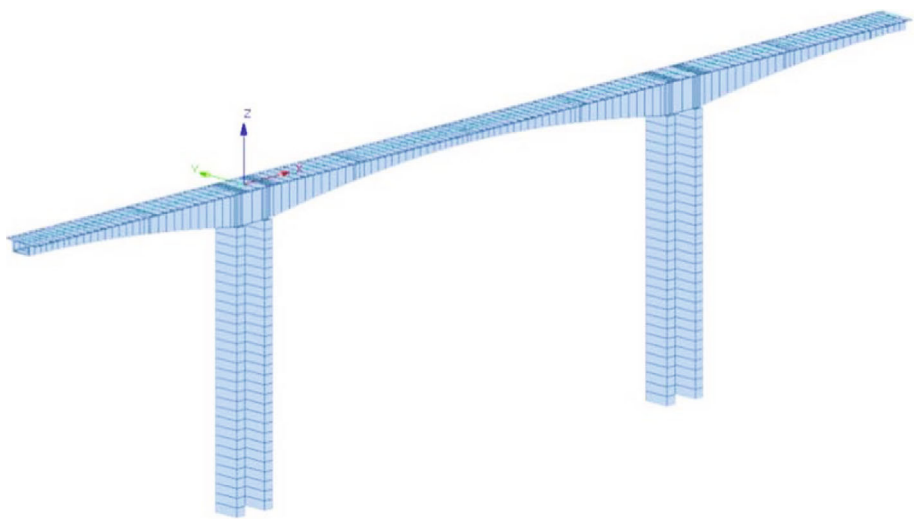

Figure 6: Finite element analysis model for continuous rigid-frame bridges.

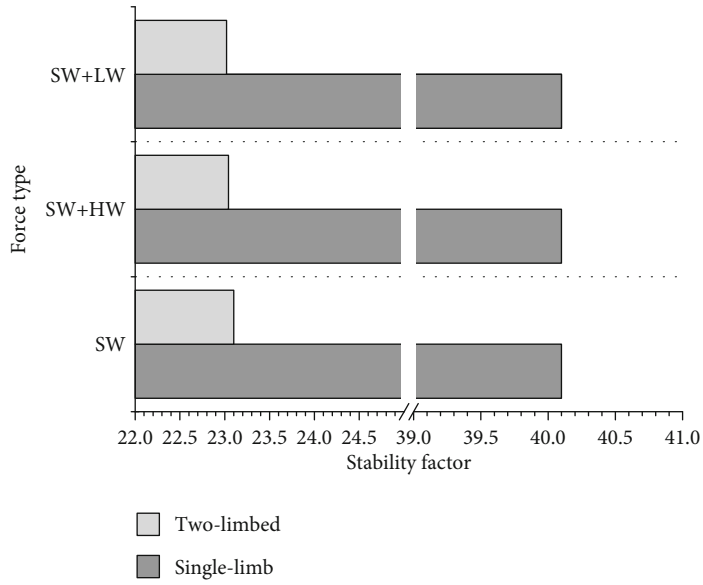

Figure 7: Stability coefficient of bridge pier under SW + LW/HW.

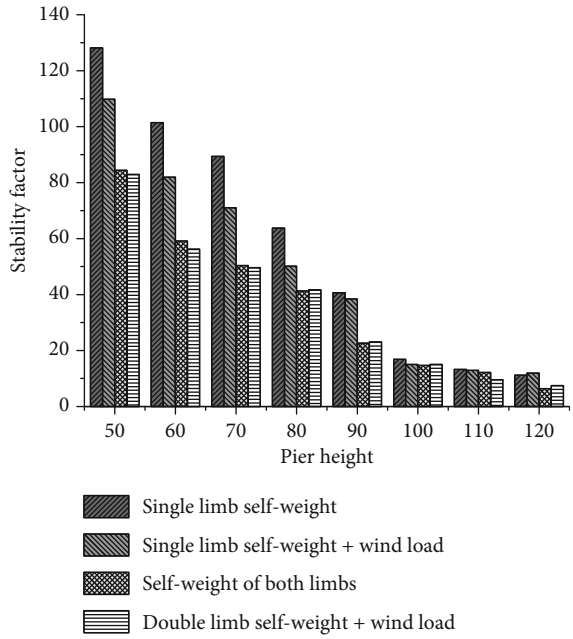

Figure 8: Change of the global stability coefficient of rigid-frame bridge with pier height.

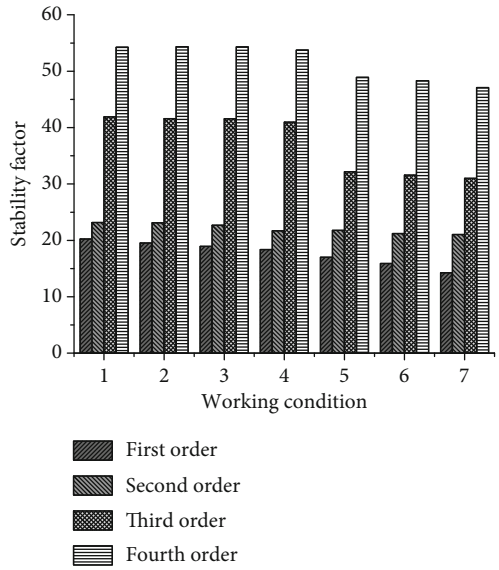

Figure 9: Variation of bridge stability coefficient under different working conditions.

resistance torque of itself M'_{Tb} and the transverse bridge horizontal force Q_b generated by the body itself. The sum of generated resistance torque and torque can be shown as

$$M''_{Tb} = Q_b \times 2r, \tag{11}$$

$$M_{Tb} = M'_{Tb} + M''_{Tb} = 2M'_{Tb} + 2rQ_b. \tag{12}$$

The value of resistance torque of double-limb thin-walled pier obtained according to the above equations is much larger than that of single-limb thin-walled pier, so the lateral torque capacity of double-limb thin-walled pier is much larger than that of single-limb thin-walled pier. This indicates that the double-limb thin-walled pier can meet the lateral wind resistance requirements of long-span continuous rigid-frame bridge in the construction process.

3.4. Global Stability Analysis of Continuous Rigid-Frame Bridges under Different Working Conditions. The analysis of static force and stiffness of continuous rigid-frame bridge structure is the basis for studying the stable mode of bridge structure under the action of external load. The failure modes of bridge under construction conditions include strength failure and instability failure. The performance of

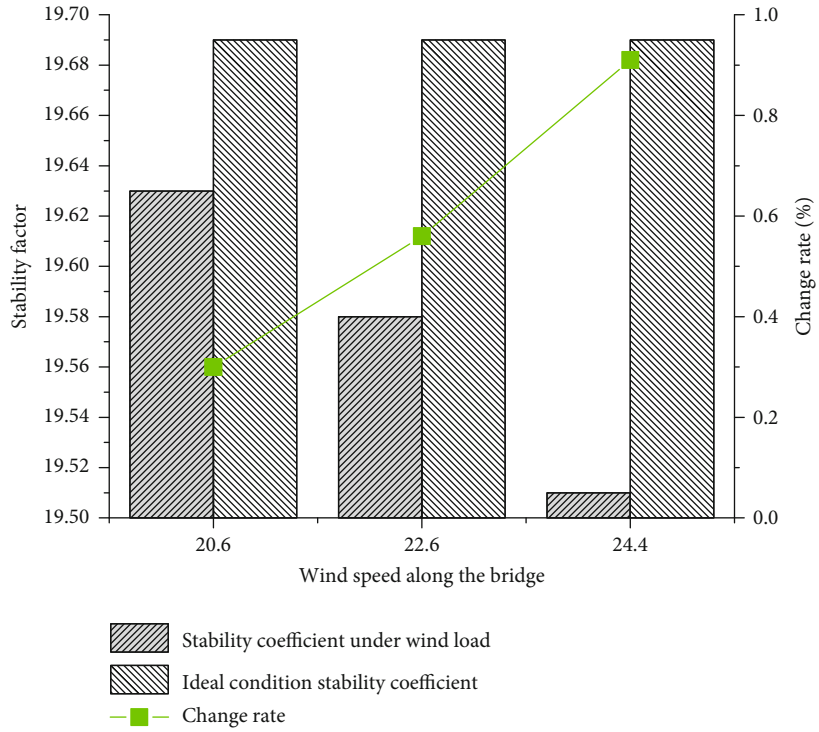

Figure 10: Comparison of the two geometric risks.

strength failure is that the internal force generated in the cross section is greater than the maximum bearing capacity of the cross-sectional material, resulting in the construction failure of the structure itself. Instability failure means that the maximum resistance of cross-sectional material is greater than the internal force of cross section, which changes the balance state of the structure and the displacement of the bridge structure, leading to the change of the bridge structure. It is necessary to determine the stability of the bridge according to the different structural forms and load forms of the continuous rigid-frame bridge firstly, to calculate the stability of the rigid-frame structure of the bridge. Then, the equilibrium equation of mechanics and displacement method is established based on this, and the corresponding critical load is solved in sequence. Ultimately, the minimum load is used as the critical value to accurately solve the buckling of the rigid-frame bridge.

In the actual environment, the maximum cantilever construction condition of the bridge structure of the continuous rigid-frame bridge is more complex, while the operation safety is low. Therefore, it is necessary to analyze the geometric nonlinear stability of the bridge under ideal state, initial defect, and wind load; to obtain the nonlinear stability safety factor and instability mode; and to further determine the influencing factors of the stability of the continuous rigid-frame bridge under wind load, initial defect, and other factors [35].

The professional bridge analysis software Midas/Civil is used to develop the structural calculation model of the continuous rigid-frame bridge, which is a three-span structure with the size of 86 + 175 + 86 m. The bridge structure involved in the model includes the main girder, pier, prestressed reinforcement, and constraint. The whole rigid-frame bridge model can be divided into 185 nodes and 174 units, the length unit is meter, and the force unit is *kN*. The beam element girder is used to model the pier of continuous rigid-frame bridge. Meanwhile, the effect of vertical and horizontal prestress on the bridge is not considered in the calculation process. Besides, the structure of continuous rigid-frame bridge is consolidated in the ground, and the two ends are the axial sliding bearings along the bridge floor. After the completion of the continuous rigid-frame bridge, the load on the bridge contains the self-weight of the bridge, the longitudinal wind load, and the transverse wind load. According to the relevant regulations, the wind load on the pier and the wind load on the transverse bridge of the bridge superstructure need to be considered in the design process of road and bridge. Figure 6 provides the established finite element analysis model for the continuous rigid-frame bridge.

4. Results and Discussion

4.1. Influence of Bridge Height on Bridge Stability. A continuous rigid-frame bridge in northwest China is selected as the research object to analyze the stability of the bridge by the Midas/Civil software. The stability coefficient and the stability mode of the bridge are obtained under three working conditions: SW (single-limb self-weight), SW + LW (self-weight + longitudinal wind), and SW + HW (self-weight + horizontal wind load), as presented in Figure 7. Figure 8 illustrates the analysis results of the stress stability of the bridge under different conditions and the global stability of the rigid-frame bridge under the condition of 50-120 m pier height under different load conditions.

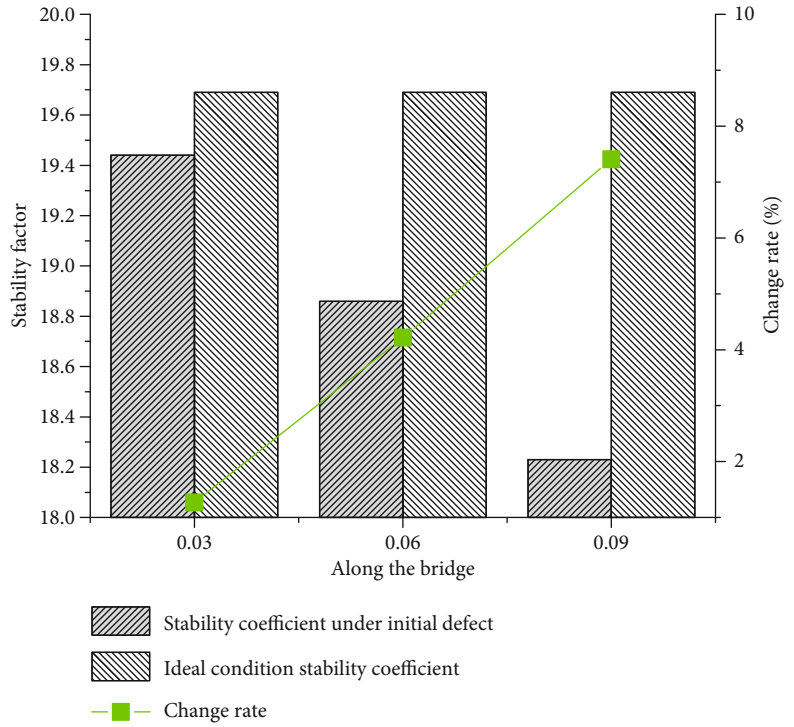

Figure 11: Stability coefficients of the bridge under different working conditions.

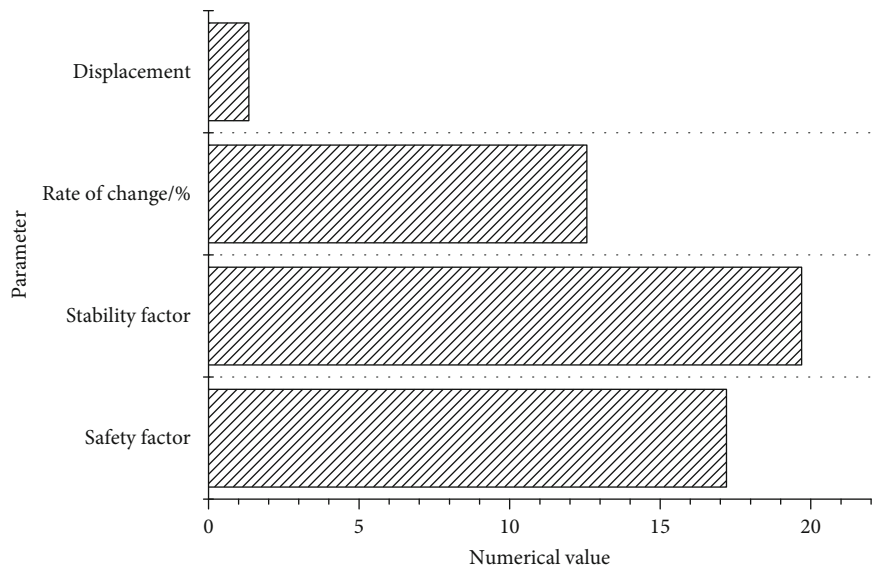

Figure 12: Comparison of two geometric nonlinear risks.

According to Figure 7, different pier heights, pier numbers, and load conditions will affect the stability of the bridge. Furthermore, under the three working conditions of SW, SW + LW, and SW + HW, the sum of stability coefficient of the bridge can meet the established requirements. From Figure 8, the stability coefficients of single-limb thin-walled pier and double-limb thin-walled pier bridges decrease with the increase of bridge height. Besides, under the same working conditions, the single-limb thin-walled pier has larger stability coefficient and better flexural performance, which can effectively control the overall stress of the structure in the construction process. Therefore, single-limb thin-walled pier should be selected as the structure of high pier rigid-frame bridge to improve the safety of traffic bridges in the concrete construction process.

4.2. Analysis of the Nonlinear Stability of Maximum Cantilever under Wind Load. Due to the geometric nonlinear characteristics of continuous rigid-frame bridge, in the ideal state, the load of the bridge includes self-weight, weight

of construction material, and the dynamic effect of hanging basket. The stability characteristic values of the bridge under different load conditions are shown in Figure 9. Additionally, Figure 10 represents the results of the longitudinal displacement of the bridge and the set nonlinear stability coefficient according to the maximum cantilever structure under the action of different wind speeds and wind pressures along the bridge direction. Moreover, the comparison results of the nonlinear stability coefficients under different wind loads and ideal conditions are exhibited in Figure 11. Besides, Figure 12 illustrates the comparison of load case and geometric nonlinear safety coefficient and stability coefficient of the bridge under the combined action of wind load and initial defects.

In Figure 9, seven working conditions are set in the construction process to test the elastic buckling of the bridge. Among the seven working conditions, the bridge has a good stability coefficient with hanging basket under the first four working conditions, and there is a drop phenomenon hanging basket under the last three working conditions. According to the results of the stability coefficient, the latter three conditions have smaller stability coefficient than the first three conditions. When in the maximum cantilever state, under normal construction conditions, the stability coefficient changes in the construction process under the latter three conditions are small, which can meet the needs of construction stability. However, it is necessary to pay attention to the influence of hanging basket on the longitudinal bending moment of the bridge and ensure that the bridge interface has sufficient bearing capacity to avoid the occurrence of bridge collapse accidents. From Figures 10 and 11, under the action of wind load, the results of the nonlinear stability of the bridge have little difference from the results under the ideal condition. The stability safety factors of the geometric nonlinear stability analysis method are 0.3% and 1.27% lower than those under the ideal condition, respectively. The reason may be that the initial displacement of the bridge caused by the wind load along the bridge is small, and thus, the effect of the large deformation produced is small. Through Figure 12, the stability safety factor of the bridge under the action of wind load and initial defect is 12.65% lower than that under the ideal state, and the stability safety factor is greatly reduced. The research results have important reference significance for ensuring the construction safety and overall stability of bridges.

5. Conclusions

The research aims to standardize the construction process of roads and bridges, improve the construction quality of long-span continuous rigid-frame bridge, and provide a stable road foundation for the development of social economy. Therefore, the continuous rigid-frame bridge is taken as the research object to analyze its development history and structural characteristics, introducing the construction process of the bridge in view of the application range of the rigid-frame bridge. Then, the thrust stiffness of two different pier structures of rigid-frame bridge, namely, single-limb thin-walled pier and double-limb thin-walled pier, is discussed under construction conditions. Finally, the analysis is performed on the stability of continuous rigid-frame bridge under the joint action of wind load and initial defects under different working conditions. These results are shown as listed as follow:

(1) The experimental results demonstrate that the pier height of the rigid-frame bridge is inversely proportional to the global stability coefficient of the bridge. Besides, the safety factor of the single-limb thin-walled pier is greater than that of the double-limb thin-walled pier

(2) Meanwhile, there is a certain gap between the stability safety factors of the nonlinear stability analysis and the ideal state in. The stability safety factor of rigid-frame bridge is greatly reduced under wind load and initial condition, which is 12.56% lower than that under the ideal state

(3) Although this study provides a reference for improving the safety and stability of road and bridge construction, there are still some deficiencies. Only the single-limb thin-walled pier and double-limb thin-walled pier are considered in the experiment, and there is insufficient analysis of relevant parameters. It is expected to further ameliorate these defects in subsequent studies to enhance the applicability of the research achievements

Data Availability

The experimental data used to support the findings of this study are included within the article.

Conflicts of Interest

The authors declare that there are no conflicts of interest regarding the publication of this paper.

References

[1] L. Gardner, "Stability and design of stainless steel structures - review and outlook," *Thin Wall Struct*, vol. 141, pp. 208–216, 2019.

[2] C. Liu, Y. Wang, X. Hu, Y. Han, X. Zhang, and L. Du, "Application of GA-BP neural network optimized by Grey Verhulst model around settlement prediction of foundation pit," *Geofluids*, vol. 2021, 16 pages, 2021.

[3] C. F. Hu and Y. M. Huang, "In-plane nonlinear elastic stability of pin-ended parabolic multi-span continuous arches," *Engineering Structures*, vol. 190, pp. 435–446, 2019.

[4] Y. Xu, Z. Zeng, Z. Wang, and H. Yan, "Seismic study of a widened and reconstructed long-span continuous steel truss bridge," *Structure and Infrastructure Engineering*, vol. 17, no. 2, pp. 191–201, 2021.

[5] H. D. Shi, F. Ji, L. Z. Shi, and S. L. Chong, "A construction technique of incremental launching for a continuous steel truss girder bridge with suspension cable stiffening chords," *Structural Engineering International*, vol. 31, no. 1, pp. 93–98, 2021.

[6] H. Gou, H. Long, Y. Bao, G. Chen, and Q. Pu, "Dynamic behavior of hybrid framed arch railway bridge under moving trains," *Structure and Infrastructure Engineering*, vol. 15, no. 8, pp. 1015–1024, 2019.

[7] J. F. Wang, J. T. Zhang, R. Q. Xu, and Z. X. Yang, "A numerically stable dynamic coefficient method and its application in free vibration of partial-interaction continuous composite beams," *Journal of Sound and Vibration*, vol. 457, pp. 314–332, 2019.

[8] A. Rossi, R. S. Nicoletti, A. S. C. de Souza, and C. H. Martins, "Numerical assessment of lateral distortional buckling in steel-concrete composite beams," *Journal of Constructional Steel Research*, vol. 172, article 106192, 2020.

[9] P. Thanopoulos, S. Louverdi, A. Spiliopoulos, and I. Vayas, "Lateral stability analysis for composite plate girder bridges," *International Journal of Streel Structures*, vol. 21, no. 2, pp. 430–441, 2021.

[10] D. N. Serras, S. D. Panagaki, K. A. Skalomenos, and G. D. Hatzigeorgiou, "Inelastic lateral and seismic behaviour of concrete-filled steel tubular pile foundations," *Soil Dynamics and Earthquake Engineering*, vol. 143, article 106657, 2021.

[11] K. Śledziewski and M. Górecki, "Finite element analysis of the stability of a sinusoidal web in steel and composite steel-concrete girders," *Materials*, vol. 13, no. 5, p. 1041, 2020.

[12] A. Miri, D. P. Thambiratnam, and T. Chan, "Thermal challenges of replacing jointed rails with CWR on steel railway bridges," *Journal of Constructional Steel Research*, vol. 181, article 106627, 2021.

[13] X. J. Gao, P. H. Duan, and H. Qian, "Dynamic response analysis of long-span continuous bridge considering the effect of train speeds and earthquakes," *Int J Struct Stab Dy*, vol. 20, no. 6, p. 2040013, 2020.

[14] J. Shi, J. Shen, G. Zhou, F. Qin, and P. Li, "Stressing state analysis of large curvature continuous prestressed concrete box-girder bridge model," *Journal of Civil Engineering and Management*, vol. 25, no. 5, pp. 411–421, 2019.

[15] W. Zheng, H. Wang, J. Li, and H. Shen, "Parametric study of superelastic-sliding LRB system for seismic response control of continuous bridges," *Journal of Bridge Engineering*, vol. 25, no. 9, p. 04020062, 2020.

[16] G. Dai, G. Chen, R. Zheng, and Y. F. Chen, "A new bilinear resistance algorithm to analyze the track-bridge interaction on long-span steel bridge under thermal action," *Journal of Bridge Engineering*, vol. 25, no. 2, p. 04019138, 2020.

[17] P. A. Montenegro, R. Calçada, H. Carvalho, A. Bolkovoy, and I. Chebykin, "Stability of a train running over the Volga river high-speed railway bridge during crosswinds," *Structure and Infrastructure Engineering*, vol. 16, no. 8, pp. 1121–1137, 2020.

[18] X. Shao, G. He, X. Shen, P. Zhu, and Y. Chen, "Conceptual design of 1000 m scale steel-UHPFRC composite truss arch bridge," *Engineering Structures*, vol. 226, article 111430, 2021.

[19] P. Górski, M. Napieraj, and E. Konopka, "Variability evaluation of dynamic characteristics of highway steel bridge based on daily traffic-induced vibrations," *Measurement*, vol. 164, article 108074, 2020.

[20] Z. Li, Z. Guo, and L. Meng, "Elastic and inelastic stability of a steel arch subjected to a crown point load under an elevated fire environment," *Engineering Failure Analysis*, vol. 123, article 105298, 2021.

[21] J. Dai, Z. D. Xu, X. J. Yin, P. P. Gai, and Y. Luo, "Parameters design of TMD mitigating vortex-induced vibration of the Hong Kong–Zhuhai–Macao Bridge deep-water nonnavigable bridge," *Journal of Bridge Engineering*, vol. 24, no. 8, p. 06019005, 2019.

[22] X. Zhou and X. Zhang, "Thoughts on the development of bridge technology in China," *Engineering-Prc*, vol. 5, no. 6, pp. 1120–1130, 2019.

[23] C. Liu, L. Du, X. Zhang, Y. Wang, X. Hu, and Y. Han, "A new rock brittleness evaluation method based on the complete stress-strain curve," *Lithosphere*, vol. 2021, p. 4029886, 2021.

[24] X. Q. Xu, X. Yang, W. Yang, X. F. Guo, and H. L. Xiang, "New damage evolution law for modeling fatigue life of asphalt concrete surfacing of long-span steel bridge," *Construction and Building Materials*, vol. 259, article 119795, 2020.

[25] L. Zhang, P. Liu, X. Yan, and X. Zhao, "Middle displacement monitoring of medium–small span bridges based on laser technology," *Structural Control & Health Monitoring*, vol. 27, no. 4, p. 2509, 2020.

[26] Z. Tian, Y. Liu, L. Jiang, W. Zhu, and Y. Ma, "A review on application of composite truss bridges composed of hollow structural section members," *J Perform Constr Fac*, vol. 6, no. 1, pp. 94–108, 2019.

[27] D. Dan, X. Yu, X. Yan, and K. Zhang, "Monitoring and evaluation of overturning resistance of box girder bridges based on time-varying reliability analysis," *J Perform Constr Fac*, vol. 34, no. 1, p. 04019101, 2020.

[28] Q. Huang, Z. Qian, L. Chen et al., "Evaluation of epoxy asphalt rubber with silane coupling agent used as tack coat for seasonally frozen orthotropic steel bridge decks," *Construction and Building Materials*, vol. 241, article 117957, 2020.

[29] X. Li, C. Gao, Y. Guo, F. He, and Y. Shao, "Cable surface damage detection in cable-stayed bridges using optical techniques and image mosaicking," *Optics and Laser Technology*, vol. 110, pp. 36–43, 2019.

[30] Y. Xia, P. Wang, and L. Sun, "Neutral axis-based health monitoring and condition assessment techniques for concrete box girder bridges," *International Journal of Structural Stability and Dynamics*, vol. 19, no. 1, p. 1940015, 2019.

[31] B. Yan, G. Zhang, Z. Han, and P. Lou, "Longitudinal force of continuously welded rail on suspension bridge with length exceeding 1000 m," *Structural Engineering International*, vol. 29, no. 3, pp. 390–395, 2019.

[32] M. Cao, C. Du, H. Guo, S. Song, X. Li, and B. Li, "Continuous network of CNTs in poly(vinylidene fluoride) composites with high thermal and mechanical performance for heat exchangers," *Composites Science and Technology*, vol. 173, pp. 33–40, 2019.

[33] Y. Zhao, J. Jiang, F. Ni, and L. Zhou, "Fatigue cracking resistance of engineered cementitious composites (ECC) under working condition of orthotropic steel bridge decks pavement," *Applied Sciences*, vol. 9, no. 17, p. 3577, 2019.

[34] L. Jiang, X. Kang, C. Li, and G. Shao, "Earthquake response of continuous girder bridge for high-speed railway: a shaking table test study," *Engineering Structures*, vol. 180, pp. 249–263, 2019.

[35] H. Zhao, Y. Ding, S. Nagarajaiah, and A. Li, "Longitudinal displacement behavior and girder end reliability of a jointless steel-truss arch railway bridge during operation," *Applied Sciences*, vol. 9, no. 11, p. 2222, 2019.